JOURNAL OF PROPULSION AND POWER
Vol. 17, No. 6, November–December 2001

Skin-Friction Measurements in a Supersonic Combustor with Crossflow Fuel Injection

H. Tanno,* A. Paull,† and R. J. Stalker‡
University of Queensland, Brisbane, Queensland 4072, Australia

Shock-tunnel experiments have been performed to measure the effect on skin-friction drag in a supersonic combustor of flow disturbances induced by hydrogen fuel injection transverse to the airstream. Constant-area, circular cross section combustors of lengths varying up to 0.52 m were employed. The experiments were done at a stagnation enthalpy of 7.2 MJ · kg^{-1} and a Mach number of 4.3, with a boundary layer that was turbulent downstream of the 0.14-m station in the combustors. Combustor skin-friction drag was measured by a method based on the stress wave force balance, the method being validated by agreement between fuel-off skin-friction drag measurements and predictions using existing skin-friction theories. When fuel was injected, it was found that the drag remained at fuel-off values. Thus, the streamwise vortices and other flow disturbances induced by the fuel injection, mixing, and combustion, which are expected to be present in a scramjet combustor, did not influence the skin-friction drag of the combustors.

Introduction

SUPERSONIC combustion ramjets offer promise for airbreathing propulsion at hypersonic flight speeds, but a number of issues remain to be resolved before their performance can be predicted with a reasonable degree of confidence. Skin-friction drag is one of these issues.

Skin friction becomes of particular importance as flight speeds increase. For instance, in Ref. 1, the results of a performance study of a hypothetical vehicle are reported in which the contribution of friction drag matches that of the wave drag at speeds above 2.5 km · s^{-1}. The component contributions to the net thrust of a scramjet are also considered in Ref. 2, where viscous effects are seen to halve the net specific impulse at 5 km · s^{-1}. A large part of this drag is contributed by the supersonic combustors because the flow density there is normally considerably higher than at any other part of the vehicle. This was illustrated during shock-tunnel experiments with a generic model of a hydrogen scramjet cruise configuration,[3] where estimates indicated that skin friction accounted for 47% of the drag measured in the fuel-off condition at 2.45 km · s^{-1} and that combustion chamber skin friction was responsible for 42% of the skin-friction drag. For missiles, studies[4] have indicated that combustion chamber skin-friction drag may be an even greater problem. Clearly, combustion chamber skin friction is an important issue.

The relatively high densities and flow speed in a scramjet combustion chamber normally result in Reynolds numbers that are high enough to ensure that boundary layers are turbulent. Substantial work has been done on the prediction of turbulent skin friction at high speeds,[5] the most popular of the resulting methods of prediction being those due to Van Driest[6] and Spalding and Chi.[7] However, these methods apply to a flat-plate boundary layer and, because the flow in a scramjet combustion chamber involves major disturbances associated with both injection and combustion of the fuel, there is doubt that these analytically based methods can be used in the scramjet combustion chamber context.

There are very few measurements of skin friction in supersonic combustors, particularly at the elevated stagnation enthalpies associated with scramjet flight. Chadwick et al.[8] have measured skin friction in supersonic combustion flowfields in vitiated blowdown facilities, obtaining results for the skin-friction coefficient that varied by more than a factor of three. Novean et al.[9] have made limited measurements in a combustion duct in an expansion tube and tentatively suggested that skin-friction coefficients might be increased by a factor of two by supersonic combustion. In both cases, the measurements were made at isolated points in the combustion duct, and it is possible that local effects were being observed that were not representative of the complete flowfield. Bowersox et al.[10] tested skin-friction gauges in supersonic combustors in shock tunnels, but not enough flowfield information was available to evaluate the results.

Shock-tunnel measurements in a supersonic combustion duct with hydrogen fuel injection parallel to the mainstream from a centrally located strut have previously been reported.[11] These measurements involved four skin-friction gauges spaced along one surface of the duct. The measured values of skin friction with combustion were found to vary from test to test but, by performing a number of tests sufficient to define a mean value with reasonable accuracy, it was found that the mean skin friction with combustion was the same as that without combustion.

It may be argued that these experiments were not representative of conditions in a practical combustion chamber because they involved only parallel injection of the fuel, whereas the demand for rapid fuel–air mixing in a practical combustion chamber leads to injection with a cross-stream component of velocity and the formation of streamwise vortices. These vortices may interact with the boundary layer and cause an increase in skin friction. Also, the experiments showed that a local measurement of skin friction in an impulsive supersonic combustion flowfield required repeated tests, coupled with a statistical analysis, to yield reasonable results, thus indicating the utility of measurements of the integrated overall skin-friction drag on a supersonic combustor as an alternative to local measurements.

The experiments reported here, therefore, had the twofold aim of determining the effect of crossflow injection on the skin friction and of measuring the integrated skin-friction drag on a supersonic combustor. Noting the importance of skin friction at high flight speeds, the experiments were performed at a stagnation enthalpy corresponding to a flight speed of 3.8 km · s^{-1}. Straight, constant-area combustors of circular cross section were chosen. The constant area had the advantage that it avoided extra experimental error involved in taking account of the integrated pressure force on the walls of the combustor in determining the skin-friction drag, and the axial symmetry provided by a circular cross section simplified interpretation of the pressure measurements. Also note that, for structural reasons,

Received 2 April 2001; revision received 24 July 2001; accepted for publication 26 July 2001.

*Visiting Scientist, Department of Mechanical Engineering; currently National Aerospace Laboratory, Kakuda Research Center, Kimigaya, Kakuda, Miyagi 981-15, Japan.

†Senior Research Fellow, Department of Mechanical Engineering.

‡Emeritus Professor, Department of Mechanical Engineering. Fellow AIAA.

a circular cross section is likely to be preferred for supersonic combustors at high enthalpies. The combustor lengths were varied and included lengths sufficient to allow almost complete combustion of the airflow with the hydrogen fuel.

The paper begins by describing the experimental arrangement, involving a description of the method of measuring the integrated skin-friction drag on a constant-area combustion duct, and follows this by consideration of the crossflow established by the method of fuel injection employed. Then the validity of the method of measuring skin-friction drag is confirmed by considering the results obtained without fuel injection, before going on to determine the effect of supersonic combustion in the duct. Discussion of the results then leads to the conclusion.

Experiment

Apparatus

The experimental apparatus is shown schematically in Fig. 1. The test flow is produced by the T4 free piston shock tunnel at the University of Queensland, operating in the shock-reflected mode. The shock tunnel is described elsewhere.[12] It supplies shock-heated air to a contoured axisymmetric nozzle of 25-mm throat diameter and 135-mm exit diameter, which produced a test flow with a core uniformity of ±5% and a diameter of approximately 100 mm (Ref. 13). As shown, the model assembly was mounted so that the intake would directly sample the test flow. The test conditions, as determined by numerical calculation of the one-dimensional nonequilibrium nozzle expansion to the measured pitot pressure, are set out in Table 1. They are similar to the test conditions of Ref. 11 and yield a shock-tunnel flow for which the level of driver gas contamination of the test flow does not rise above 10% for at least 2.2 ms after shock reflection at the end of the shock tube. The flow starting process was complete within 0.8 ms, and so the test period was taken as the 1 ms beginning 1.0 ms after shock reflection. This corresponded to the time taken for the airflow to pass a distance equal to 6.3 times the length of the longest combustor tested.

Table 1 Airflow Test Conditions

Quantity	Units	Value	Estimated error, %	Reproducibility, %
Stagnation enthalpy	$MJ \cdot kg^{-1}$	7.2	+4, −8	±2
Nozzle reservoir pressure	MPa	31	±5	±3.3
Mach number	——	4.3	±5	±0.6
Static temperature	K	1600	+4, −8	±2
Static pressure	kPa	85	±8	±3
Density	$kg \cdot m^{-3}$	0.18	±13	±2.5
Velocity	ms^{-1}	3300	+2, −4	±0.7
Pitot pressure	MPa	1.7	±6	±3
Reynolds number per meter	——	1.0×10^7	±14	±4.7

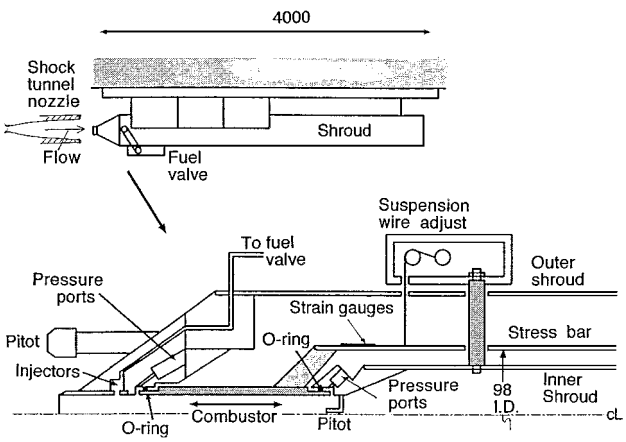

Fig. 1 Model assembly (dimensions in millimeters).

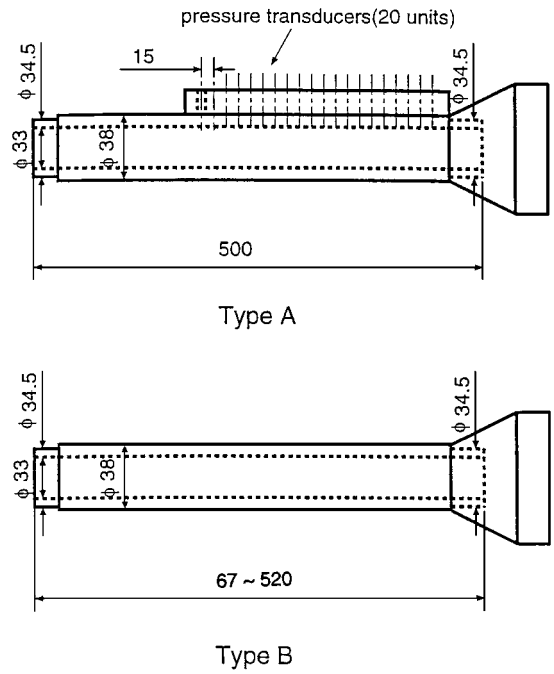

Fig. 2 Combustor model geometries (dimensions in millimeters): type A is for pressure measurement, type B is for skin-friction force measurement.

The supersonic combustors consisted of a constant-area duct with a circular cross section 33 mm in diameter. The drag force on a combustor was measured by attaching it to the stress bar of a stress wave force balance, as shown in Fig. 1. The principle of the stress wave force balance was set out in Ref. 14, and it has been used in a number of experimental programs to measure drag force on shock-tunnel models, for example, see Ref. 12. Here the stress bar was a thin-walled brass tube, of inner diameter 98 mm and 2.8 m long, that was suspended with thin steel wires and protected from the external flow by the outer shroud and from the internal flow (which passes through the combustor) by the inner shroud. The shrouding was completed by the front conical section of 30-deg semivertex angle, leading to the intake. The arrangement was intended to ensure that transmission to the stress bar of extraneous forces, other than the force acting on the internal surface of the combustor, was minimized. To further this objective, the combustors were designed with a short section at each end of 0.75-mm wall thickness, as shown in Figs. 1 and 2. O-ring seals were made between the combustor and the shroud assembly close to the leading and the trailing edge of the combustor, the contact between the O-rings and the outer surface of the combustor being such that the combustor experienced negligible O-ring friction. Thus, the only extraneous force acting on the combustor was that due to the pressure difference, between the leading and the trailing edge of the combustor, acting on the surface area afforded by the 0.75-mm wall thickness at each end. A correction was made for this force by taking the mean of the pressures measured by an array of six pressure ports at the leading edge and the trailing edge, using the difference of the means to calculate the extraneous force, and then subtracting this from the force measured with the stress wave force balance. This led to a maximum correction of approximately 10% of the measured force. Of course, this correction required that only a small gap existed between each end of the combustor and the shroud assembly and, as will be seen later, it fails if this condition is not satisfied.

Two types of combustors were used, as shown in Fig. 2. Type A was used to obtain combustion chamber pressure distributions and was instrumented with PCB™ quartz piezoelectric pressure transducers, whereas type B, which was used to measure the skin-friction force, was manufactured of aluminium in combustion chamber lengths of 67, 120, 220, 320, 420, 500, and 520 mm. The conical attachment between the combustion chamber and the stress bar is also shown schematically in Fig. 2.

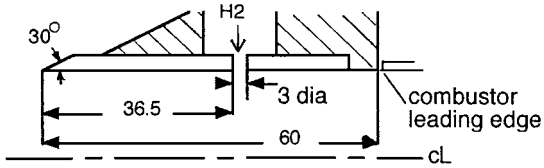

a) Inlet duct showing location of fuel injection orifices

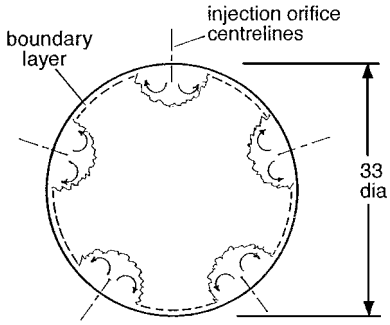

b) Cross section of flow pattern 100 mm downstream of injection (ϕ = 1)

Fig. 3 Hydrogen fuel injection (dimensions in millimeters).

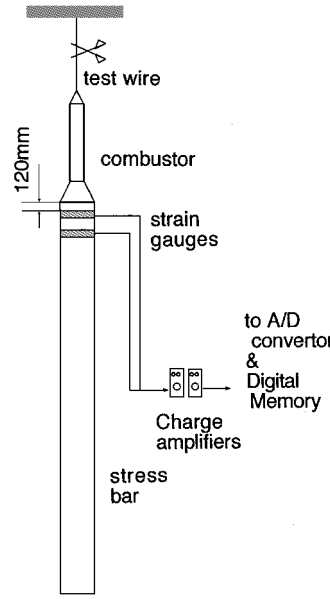

Fig. 4 Wire-cutting calibration test.

Inlet Section and Injectant Flow Patterns

A detail of the duct inlet section is shown in Fig. 3a. There were five fuel injection orifices, each 3 mm in diameter, equally spaced about the circumference of the duct at 38 mm from the leading edge. Room-temperature hydrogen was supplied to the injection orifices by a fast-acting fuel valve,[15] the hydrogen flow rate being monitored by two piezoelectric pressure transducers located in the manifold downstream of the valve. The measured pressures were such as to assure sonic flow at the injection orifices. Precalibration of the system allowed the hydrogen flow rate to be determined from the pressure measurements, and this, together with the test flow properties set out in Table 1, yielded the equivalence ratio ϕ, with an accuracy of $\pm 16\%$.

Figure 3b is the crossflow pattern 100 mm downstream of injection at $\phi = 1$. It was obtained by assuming that the flow from each orifice was identical to that obtained with a single orifice in a flat surface. The hydrogen penetration distance into the mainstream was estimated from Refs. 16 and 17, using the ratio of momentum flux per unit area, that is, ρu^2, in the hydrogen jet to that in the mainstream as a correlating parameter. This correlation is independent of the injectant molecular weight and the freestream Mach number.[16] The lateral hydrogen penetration was obtained in the same manner. It represents the lateral extent of each of the two vortices[17,18] induced by the jet from the orifice. The broken line in Fig. 3b shows the calculated edge of the boundary layer (which is laminar at this station) in the absence of the jets and demonstrates that the hydrogen penetrates to well beyond the boundary layer.

For stations farther downstream, the injection flow patterns grow and merge, and mixing and combustion of the hydrogen generates a rise in pressure. As will be seen hereafter, this pressure rise begins less than 200 mm from injection, a downstream distance corresponding to 6.1 duct diameters, and approaches the fully mixed and burned equilibrium value by 400 mm, a distance corresponding to 12.1 duct diameters. Such length to diameter ratios are expected to be typical of full-scale scramjet combustors at the flow conditions of these experiments and, in combination with the hydrogen penetration distances illustrated in Fig. 3b, indicate that the mixing and combustion obtained in these experiments was typical of a practical scramjet combustor. Thus, the streamwise vortices caused by fuel injection, which may interact with the boundary layer to cause an increase in skin friction are, at least qualitatively, correctly modeled in the experiments.

Calibration of Stress Wave Force Balance

Piezoelectric film strain gauges were attached to the stress bar 120 mm from the model attachment collar, as shown in Fig. 1. They encircled the stress bar to cancel the effects of any bending that might occur, and, therefore, they responded only to longitudinal stress waves. The time history of these stress waves is a function of the loads applied to the model, and the relation between the two can be written as

$$x(t) = \int_0^t g(t-\tau) f(\tau)\, d\tau \qquad (1)$$

where $x(t)$ is the measured signal, $f(t)$ the input signal due to the applied loads, and $g(t)$ an impulse response function that relates $x(t)$ and $f(t)$. Because the system is elastic, and, therefore, linear, the impulse response function can be determined by applying a step function load to the system and measuring the output signal. With $g(t)$ thus determined, numerical deconvolution procedures allow $f(t)$ to be determined from $x(t)$. More detail on this procedure can be found in Ref. 14.

To apply a step load, a wire-cutting calibration test was used. As shown in Fig. 4, the combustor and force balance assembly (without the shroud) was suspended by a fine wire attached to the combustor, and the wire was suddenly severed. The strain gauges recorded the output signal and, by relating it to the change in the wire load, that is, the weight of the assembly, the impulse response function could be determined. Both the process of calibration and of numerical deconvolution of the measured signal in a test were simplified by using a long stress bar because the arrival of stress wave reflections from the downstream end of the bar was delayed until the test time was over.

Data Recording

Data were recorded and stored on a 12-bit transient digital data store with a sampling time of 1 μs. Pressure transducer outputs were recorded through two-times multiplexers, resulting in a sampling time of 2 μs. The force balance strain-gauge outputs were stored directly, with the numerical deconvolution performed after each test to yield the force record.

Results and Discussion

Pressure Measurements

Figure 5 shows pressure distributions measured in the type A combustor, normalized by the measured pressure at the combustor leading edge. This pressure was 75 ± 6 kPa for $\phi = 0$, rising to 95 ± 8 kPa for $\phi = 1.5$. Figure 5a displays examples of the pressure distribution obtained at intervals of 0.1 ms during the 1 ms test time, both with and without the introduction of fuel. The flow disturbances seen are attributed to the presence of the injection ports, the fuel injection itself, and to the gap between the shroud assembly and

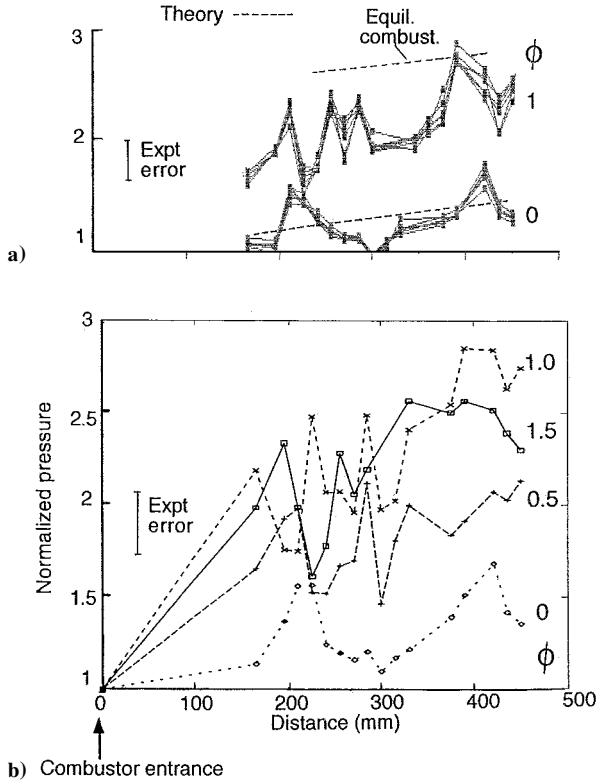

Fig. 5 Wall pressure distributions: a) variation during test time together with theoretical affects of boundary growth and complete combustion and b) effect of fuel flow.

the leading edge of the combustor, as well as a possible slight misalignment of the duct with respect to the test flow direction. Though there is some relatively small variation of the pressure distributions during the test time, it is seen that the overall distribution remains unchanged, indicating that the flow is essentially steady during this period. Also note that the pressure distributions of Figs. 5a and 5b, at $\phi = 1$ and 0, were not taken from the same test. Though there is some variation in detail between the two sets of data at $\phi = 1$, possibly due to shot-to-shot variation in the hydrogen mass flow, it can be seen that overall shot-to-shot reproducibility is essentially maintained.

The increase in pressure due to the growth of the boundary layer in the absence of fuel injection is shown by the broken line at $\phi = 0$ in Fig. 5a. This was calculated by using the predicted incompressible boundary-layer thickness, modified by the reference enthalpy method,[19] and combining this with a one-seventh power law velocity profile and a linear variation of stagnation enthalpy with velocity to estimate the displacement thickness. The measured pressure distribution at $\phi = 0$ is not inconsistent with this calculation.

As shown in Fig. 1, pitot pressure measurements were made at the exit of the type A combustor and, when these were combined with the static pressure measurements, they indicated a Mach number that fell from a value of 3.5 in the absence of hydrogen fuel addition to a value of 1.8 when the fuel was added at an equivalence ratio of 1.5. Thus, supersonic combustion took place throughout the experiments. The expected increase in pressure due to complete combustion at $\phi = 1$ in a constant-area duct with the final combustion products in chemical equilibrium has been calculated[20] and added to the rise in pressure due to boundary-layer growth at $\phi = 1$ in Fig. 5a. Measured pressures approach this line between the 200- and 400-mm stations, indicating that substantially complete combustion had occurred at these distances from injection. Also, Fig. 5b shows that the pressure rise increased as the fuel flow increased up to an equivalence ratio of one, where it appears that it may have reached a plateau. This is further evidence that, in addition to being supersonic, the combustion was essentially completed within the length of the duct.

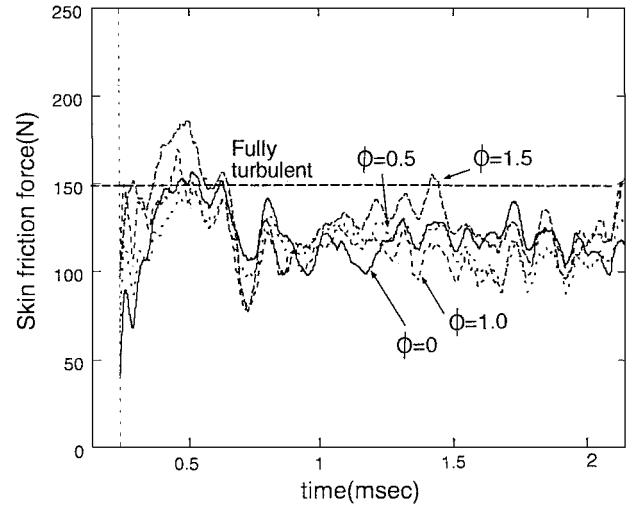

Fig. 6 Records of axial force on 520-mm combustor.

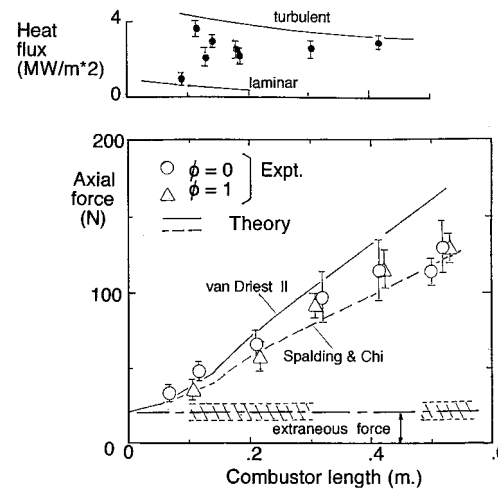

Fig. 7 Effect of combustor length on skin-friction drag and comparison with fuel-off theoretical predictions.

Force Measurements

Deconvolved records of the axial force on the 520-mm type B combustor are shown in Fig. 6. Time is measured from the moment of shock reflection in the shock tube. It is seen that there was no distinguishable effect on the axial force as the hydrogen fuel equivalence ratio was increased from 0 to 1.5. The estimated[6] level expected for the axial force due to skin friction with a fully turbulent boundary layer is also shown on Fig. 6. The measured levels are approximately 75% of this level, indicating that all or most of the forces measured were due to skin friction.

Identification of the measured axial force with skin friction was carried further by measurements on combustion ducts of different lengths, at equivalence ratios of zero and unity, with the results shown in Fig. 7. It can be seen that, as in Fig. 6, fuel injection does not significantly influence the measured drag force. However, it can also be seen that the drag does not approach zero as the combustor length approaches zero, indicating that a residual extraneous force on the combustor remains. Inspection of the model on completion of these experiments revealed that a design detail fault with the type B combustors caused a 5-mm gap to form between the leading edge of the combustor and the trailing edge of the inlet section, permitting the possibility of leakage from the airflow that would be sufficient to generate the extraneous forces required. The fault was rectified and the 220- and 420-mm combustors were tested again at $\phi = 0$, yielding force measurements of 48 ± 4 N and 95 ± 5 N, respectively. The corresponding measurements in Fig. 7 are 67 and 117 N, respectively, indicating an extraneous force of 19 and 22 N, respectively.

This will apply to all tests with type B combustors. Thus, the average value of the extraneous force is taken to be 21 N and is plotted as the broken line in Fig. 7 to yield an effective zero for the skin-friction force measurements. The uncertainty of ±5 N obtained in the measurements with the rectified combustors is represented by the crosshatched zone in Fig. 7, and this may be combined with the uncertainty indicated by the error bars for individual points to obtain the uncertainty in the final skin-friction force measurements.

Comparison with Fuel-off Skin-Friction Predictions

With the extraneous force accounted for, the skin-friction drag measurements with no fuel injection can be compared with predictions using established methods. These calculations of the skin-friction drag will depend on the location of the station at which boundary-layer transition occurs. Heat transfer measurements in the shock tunnel at a Mach number of 6 (Ref. 21) and the unit Reynolds number of the present experiments indicated that transition was completed at a Reynolds number Re_x of 2.7×10^6. The different model configuration and Mach number of the present experiments suggested that this value should be checked, and so measurements were made with thermocouple heat transfer gauges situated in the wall of duct A. The results, shown at the top of Fig. 7, indicate that transition is completed approximately 140 mm downstream of the combustor leading edge and, noting that the length of the inlet section is 60 mm, the unit Reynolds number of Table 1 yields a Reynolds number at the end of transition of 2.0×10^6, a value which is only a little less than that of Ref. 21.

Thus, the boundary layer is turbulent downstream of the 140-mm station. The virtual origin for turbulent boundary-layer calculations, assumed to be at 82.5% of the distance to transition,[22] is located at the 105-mm station. The calculations of the skin-friction drag were made using the methods of both Van Driest[6] and Spalding and Chi[7] for the skin friction in the turbulent boundary layer. In the transition region, assumed to run from the 60-mm station to the 140-mm station,[21] the skin friction is assumed to vary linearly from the laminar to the turbulent value. In the laminar region, the reference enthalpy method is used in determining skin friction.[19]

The growth of the boundary layer in the duct leads to constriction of the flow, with a consequent increase in the dynamic pressure, as well as the increase in static pressure that has already been noted. To take account of the effect of this dynamic pressure increase on the skin friction, the normalized pressure of Fig. 5 was represented by a distribution that increased linearly from 1.0 to 1.5 over 0.5 m of duct length, and the associated increase in dynamic pressure was calculated by assuming isentropic flow with a ratio of specific heats of 1.3. This increase was then combined with the skin-friction coefficient, multiplied by the duct perimeter, and the result integrated over the duct length to obtain the resulting increase in skin-friction drag. It was found that the proportional increase varied linearly with the duct length, reaching a maximum of 16% for the 520-mm duct. This was incorporated into the calculations for Fig. 7.

Comparing the results of these calculations of total skin-friction force with the experimental measurements in Fig. 7, it is seen that the measured axial force (minus the extraneous force of 21 N) falls between the skin-friction predictions made according to Van Driest[6] and Spalding and Chi.[7] This is in accord with Ref. 23, where it was found that flat-plate skin friction, measured in the shock tunnel, also tended to fall between predictions made by the same two methods. Thus, to within the accuracy with which skin friction can be predicted, the measured and predicted values of the skin-friction force are consistent, confirming the efficacy of this method of skin-friction force measurement. To within the same accuracy, the measurements with fuel added are indistinguishable from those without fuel addition.

Thus, the measurements indicate that mixing and combustion, with varying amounts of fuel addition, does not affect the skin-friction drag of the 520-mm combustor. The same applies when the length of the combustor is varied at an equivalence ratio of one, indicating that the axial distribution of skin friction is also unaffected, in spite of the presence of the pressure disturbances evident in Fig. 5. It is clear that the generation of flow conditions typical of those likely to be found in a practical scramjet combustor yields the same result as Ref. 11, namely, that the mean skin friction is not affected by supersonic combustion.

Conclusions

Shock-tunnel experiments have been conducted to measure the effect of transverse fuel injection on the skin-friction drag experienced by a simple, constant-area supersonic combustor of circular cross section. The experiments were done at a precombustion freestream temperature of 1600 K, a Mach number of 4.3, and a static pressure of 85 kPa. Hydrogen fuel injection took place normal to the mainstream flow, through five sonic orifices equally spaced on the perimeter of the duct, producing the streamwise vortices and pressure disturbances that are expected to be characteristic of typical scramjet combustors. Pressure distributions indicated that vigorous combustion took place at equivalence ratios from 0.5 to 1.5.

An adaptation of the stress wave force balance was used to measure the total skin-friction drag on the combustors. Tests on a series of combustors of varying length showed that, in the absence of fuel injection, the measured drag was consistent with predictions of existing skin-friction theories. This confirmed the efficacy of this method of measuring the integrated skin-friction drag. When fuel was injected, it was found that the skin friction was not measurably affected, both when the equivalence ratio was varied with a fixed combustor length and when the combustor length was varied with a fixed equivalence ratio. It is concluded that, in spite of the streamwise vortices and other flow disturbances introduced, the overall skin-friction drag is not significantly affected by transverse fuel injection. Because these disturbances are thought to be typical of those in a working scramjet combustor, the results, together with similar results for parallel injection in Ref. 11, indicate that the level of skin-friction drag in such a combustor would not be affected by injection, mixing, and burning of the fuel.

Acknowledgments

This research was funded by the Australian Research Council and the Japan Science and Technology Corporation. The authors would like to thank S. Lentz for performing the measurements on the rectified 220- and 420-mm combustors.

References

[1] Billig, F. S., "Overview of Propulsion Performance," *Future Aerospace Technology in the Service of the Alliance, Vol. 3, Sustained Hypersonic Flight*, CP-600, AGARD, 1997, pp. C33-1–C33-11.

[2] Erdos, J. I., "Scramjet Testing in Shock-Heated Tunnels," *Proceedings of the 21st International Symposium of Shock Waves*, edited by A. F. P. Houwing, Australian National Univ., Panther Pub. and Print., Fyshwick, Australia, 1997, pp. 1125–1130.

[3] Stalker, R. J., and Paull, A., "Experiments on Cruise Propulsion with a Hydrogen Scramjet," *Aeronautical Journal of the Royal Aeronautical Society*, Vol. 102, No. 1011, 1998, pp. 37–43.

[4] Starky, R., and Lewis, M. J., "Performance of Hypersonic Waverider Missiles Using Multiple Scramjets," AIAA Paper 99-4953, June 1999.

[5] White, F. W., *Viscous Fluid Flow*, 2nd ed., McGraw–Hill, New York, 1991, p. 549.

[6] Van Driest, E. R., "The Problem of Aerodynamic Heating," *Aeronautical Engineering Review*, Vol. 15, No. 10, 1956, pp. 26–41.

[7] Spalding, D. B., and Chi, S. W., "The Drag of a Compressible Turbulent Boundary Layer on a Smooth Flat Plate With and Without Heat Transfer," *Journal of Fluid Mechanics*, Vol. 18, 1964, pp. 117–143.

[8] Chadwick, K. M., DeTurris, D. J., and Schetz, J. A., "Direct Measurements of Skin Friction in Supersonic Combustion Flow Fields," *Journal of Engineering for Gas Turbines and Power*, Vol. 115, No. 3, 1993, pp. 507–514.

[9] Novean, M. G., Schetz, J. A., and Bowersox, R. D. W., "Direct Measurements of Skin Friction in Complex Supersonic Flows," AIAA Paper 97-0394, Jan. 1997.

[10] Bowersox, R. D. W., Schetz, J. A., Chadwick, K., and Deiwert, S., "Technique for Direct Measurement of Skin Friction in High Enthalpy Impulsive Scramjet Flowfields," *AIAA Journal*, Vol. 33, No. 7, 1995, pp. 1286–1291.

[11] Goyne, C. P., Stalker, R. J., and Paull, A., "Shock-Tunnel Skin-Friction Measurement in a Supersonic Combustor," *Journal of Propulsion and Power*, Vol. 15, No. 5, 1999, pp. 699–705.

[12]Paull, A., Stalker, R. J., and Mee, D. J., "Experiments on Supersonic Combustion Ramjet Propulsion in a Shock Tunnel," *Journal of Fluid Mechanics*, Vol. 296, Aug. 1995, pp. 159–183.

[13]Jacobs, P. J., and Stalker, R. J., "Mach 4 and Mach 8 Axisymmetric Nozzles for a High Enthalpy Shock Tunnel," *Aeronautical Journal of the Royal Aeronautical Society*, Vol. 95, No. 949, 1991, pp. 324–334.

[14]Sanderson, S. R., and Simmons, J. M., "Drag Balance for Hypervelocity Impulse Facilities," *AIAA Journal*, Vol. 29, No. 12, 1991, pp. 2185–2191.

[15]Morgan, R. G., and Stalker, R. J., "Fast Acting Hydrogen Valve," *Journal of Physics E: Scientific Instruments*, Vol. 16, No. 2, 1983, pp. 205–207.

[16]Gruber, M. R., Nejad, A. S., Chen, T. H., and Dutton, J. C., "Mixing and Penetration Studies of Sonic Jets in a Mach 2 Freestream," *Journal of Propulsion and Power*, Vol. 11, No. 2, 1995, pp. 315–323.

[17]McDaniel, J. C., and Graves, J., Jr., "Laser-Induced-Fluorescence Visualization of Transverse Gaseous Injection in a Nonreacting Supersonic Combustor," *Journal of Propulsion and Power*, Vol. 4, No. 6, 1988, pp. 591–597.

[18]Zukoski, E. E., and Spaid, F. W., "Secondary Injection of Gases into a Supersonic Flow," *AIAA Journal*, Vol. 2, No. 10, 1964, pp. 1689–1696.

[19]Eckert, E. R. G., "Engineering Relations for Friction and Heat Transfer to Surfaces in High Velocity Flow," *Journal of the Aeronautical Sciences*, Vol. 22, No. 8, 1955, pp. 585–587.

[20]Heiser, W. H., and Pratt, D. T., *Hypersonic Airbreathing Propulsion*, edited by J. S. Przemieniecki, AIAA Education Series, AIAA, Washington, DC, 1994, p. 318.

[21]He, J., and Morgan, R. G., "Transition of Compressible High Enthalpy Boundary Layer Flow over a Flat Plate," *Aeronautical Journal of the Royal Aeronautical Society*, Vol. 98, No. 972, 1994, pp. 25–34.

[22]Cary, A. M., and Bertram, M. H., "Engineering Prediction of Turbulent Skin Friction and Heat Transfer in High-Speed Flow," NASA TN D-7507, 1974.

[23]Goyne, C. P., "Skin Friction Measurements in High Enthalpy Flows at High Mach Number," Ph.D. Dissertation, Mechanical Engineering Dept., Univ. of Queensland, Brisbane, Queensland, Australia, May 1999.